EngOpt 2012 – 3rd International Conference on Engineering Optimization
Rio de Janeiro, Brazil, 01 - 05 July 2012.

Model Predictive Control for Vehicle Yaw Stability

Mooryong Choi and Seibum Choi

Department of Mechanical Engineering, KAIST, 335 Gwahagno, Yuseong-gu, Daejeon, 305-701, Korea

1. Abstract
Yaw stability of an automotive vehicle in a turn is critical to the overall stability of the vehicle. In this paper, we present a method of vehicle stability control (VSC) based on Model Predictive Control (MPC). Conventional VSCs work passively as they detect excessive yaw rate or slip angle of a vehicle. However, in many cases, when excessive yaw rate or slip angle of a vehicle is detected, the vehicle is already in unstable states. Using the MPC scheme, the proposed controller can actuate brakes to generate correction moment in advance of vehicle being unstable by predicting vehicle movement of several hundred milliseconds ahead. The differences of desired vehicle states from the bicycle model and the estimated vehicle state are minimized by applying the MPC scheme. The performance of the proposed method is evaluated using the vehicle dynamics software CARSIM.

2. Keywords: Vehicle Dynamics, Yaw Stability, Model Predictive Control (MPC), Optimization

3. Introduction
Various types of Electronic Stability Control (ESC) have been developed by many researchers [1][2][3]. Basically, these ESC algorithms are activated to exert correction moment when excessive differences of actual and desired yaw rates or immoderate side slip angles are detected. However, when excessive side slip angles or excessive differences of actual and desired yaw rates are detected, in many cases, vehicles are already in unstable states. Since vehicle in unstable states tend to quickly spin out or bounce out from its desired trajectory, small delay of ESC actuation can be followed by fatal accidents. To overcome this drawback of conventional ESC, this paper focuses on development of a new ESC algorithm based on MPC scheme. First, bicycle model is designed to capture the characteristics of vehicle lateral dynamics. The initial cornering stiffness is used to generate desired yaw rate. On-line cornering stiffness adaptation is performed using the tire model [4]. The MPC scheme generates the corrective yaw moment to minimize the corrective yaw moment and the difference between the desired yaw rate and actual yaw rate.

4. Development of Yaw Stability Controller based on MPC

4.1. Vehicle Lateral Dynamics Modeling
In this section, a simple bicycle model with dynamic tire model is used to generate desired yaw rate. This bicycle model as shown in Fig.1 describes vehicle lateral dynamics.

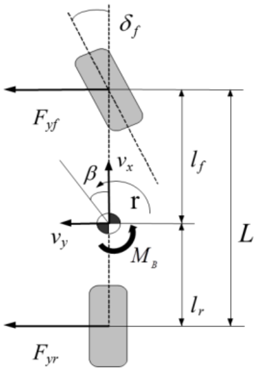

Figure 1. Bicycle Model

The equations of motion for the bicycle model are as follows:

$$mv_x(\dot{\beta}+r) = F_{yf} + F_{yr} \tag{1}$$

$$I_z\dot{r} = l_f F_{yf} - l_r F_{yr} \tag{2}$$

Where

$$F_{yf} = C_f \alpha_f$$
$$F_{yr} = C_r \alpha_r$$
$$\alpha_f = \delta_f - \left(\beta + \frac{l_f \cdot r}{v_x}\right)$$
$$\alpha_r = -\beta + \frac{l_r \cdot r}{v_x}$$

Dynamic tire model as defined in [5] can be obtained as follows:

$$\tau \dot{F}_{y\_lag} + F_{y\_lag} = F_y \qquad , \tau = \frac{C_\alpha}{KV_x} \qquad , K = \left. \frac{\partial F_y}{\partial y} \right|_{y=0} \qquad , L = \frac{C_\alpha}{K} \cong 1.5m$$

The lagged lateral tire forces can be defined as follows:

$$\tau \dot{F}_{y\_lag} + F_{y\_lag} = F_{yf} ,$$
$$\tau \dot{F}_{yr\_lag} + F_{yr\_lag} = F_{yr}$$

Using the first order dynamic tire model and laplace transform, front and rear lateral tire force equations can be replaced by the follows:

$$mv_x (s\beta + r) = F_{yf\_lag} + F_{yr\_lag}$$
$$I_z sr = l_f F_{yf\_lag} - l_r F_{yr\_lag}$$
,

As a result, the following state space form equation can be obtained

$$\dot{X} = AX + B\delta \tag{3}$$

$$X = \begin{bmatrix} \beta & \dot{\beta} & r & \dot{r} \end{bmatrix}^T$$

$$A = \begin{bmatrix} 0 & 1 & 0 & 0 \\ -\frac{C_f + C_r}{\tau m v_x} & -\frac{1}{\tau} & \left(\frac{C_r l_r - C_f l_f}{\tau m v_x^2} - \frac{1}{\tau} \right) & -\frac{1}{\tau} \\ 0 & 0 & 0 & 1 \\ \frac{C_r l_r - C_f l_f}{\tau I_z} & 0 & -\frac{C_f l_f^2 + C_r l_r^2}{\tau I_z v_x} & -\frac{1}{\tau} \end{bmatrix}$$

$$B = \begin{bmatrix} 0 \\ \frac{C_f}{\tau m v_x} \\ 0 \\ \frac{C_f l_f}{\tau I_z} \end{bmatrix}$$

By using the dynamic tire model, the bicycle model can be reformed to have the four states including derivatives of yaw rate and side slip angle and lagged characteristics of tire forces to better describe vehicle lateral dynamics.

4.2 Tire Model

In a regular bicycle model, the cornering stiffnesses C_f , C_r are set to be constants. However, as slip angles increase or tire longitudinal forces are applied, those cornering stiffnesses decrease. To take these phenomenon into account, the combined longitudinal and lateral brushed tire model [t] which is simple enough to be run in real-time while complicated enough to capture the tire nonlinear characteristics is used. The equations of the tire model is as follow:

$$F_x = \frac{C_x \left(\frac{\kappa}{1+\kappa} \right)}{f} F \tag{4}$$

$$F_y = -\frac{C_\alpha \left(\frac{\tan \alpha}{1+\kappa} \right)}{f} F \tag{5}$$

Where

$$
\begin{aligned}
F &= \begin{cases} f - \frac{1}{3\mu F_z} f^2 + \frac{1}{27\mu^2 F_z^2} f^3 & \text{if} \quad f \le 3\mu F_z \\ \mu F_z & \text{else} \end{cases} \\
f &= \sqrt{C_x^2 \left(\frac{\kappa}{1+\kappa}\right)^2 + C_\alpha^2 \left(\frac{\tan\alpha}{1+\kappa}\right)^2} \\
\kappa &= \frac{R_e\omega - V_{xt}}{V_{xt}}
\end{aligned}
$$

The following parameters are identified in real-time using the linearized recursive least squares method [] in real-time.

$$\mu,\ C_x,\ C_\alpha$$

4.3. Linearized Tire Model

Since we have the nonlinear tire model which is identified in real-time, the nonlinear tire characteristics can be reflected to the bicycle model by linearizing the tire force curve at current slip angle.

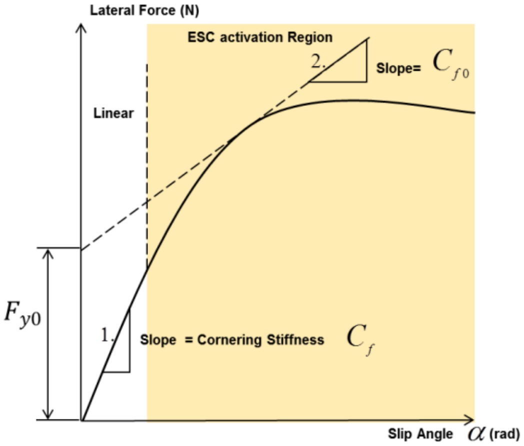

Figure 2. Generic Lateral Tire Force vs Slip Angle Curve

$$F_y = C_f \alpha \tag{6}$$

$$F_y = C_{f0} \alpha + F_{y0} \tag{7}$$

The tire force can be expressed as in (7) by linearizng the tire model at the current slip angle. Using (7) for the front and rear tire forces, the bicycle model with dynamics tire model can be modified as follow:

$$\dot{X} = A_0 X + B_0 \delta + C_0 + D_0 M_c \tag{8}$$

$$
A_0 = \begin{bmatrix}
0 & 1 & 0 & 0 \\
-\dfrac{C_{f0} + C_{r0}}{\tau m v_x} & -\dfrac{1}{\tau} & \left(\dfrac{C_{r0} l_{r0} - C_f l_f}{\tau m v_x^2} - \dfrac{1}{\tau}\right) & -\dfrac{1}{\tau} \\
0 & 0 & 0 & 1 \\
\dfrac{C_{r0} l_r - C_{f0} l_f}{\tau I_z} & 0 & -\dfrac{C_{f0} l_f^2 + C_{r0} l_r^2}{\tau I_z v_x} & -\dfrac{1}{\tau}
\end{bmatrix}
$$

$$B_0 = \begin{bmatrix} 0 \\ \frac{C_{f0}}{\tau m v_x} \\ 0 \\ \frac{C_{f0} l_f}{\tau I_z} \end{bmatrix} \quad C_0 = \begin{bmatrix} 0 \\ \frac{F_{0f} + F_{0r}}{\tau m v_x} \\ 0 \\ \frac{l_f F_{0f} - l_r F_{0r}}{\tau I_z} \end{bmatrix} \quad D_0 = \begin{bmatrix} 0 \\ 0 \\ 0 \\ \frac{1_z}{\tau I_z} \end{bmatrix}$$

M_c is the corrective moment. C_0 is the additional term due to the linearization. (3) is used to generate the desired yaw rate, whereas (8) is used to calculate the corrective yaw moment in the MPC scheme.

4.3. Calculation of Correction Moment based on Model Predictive Control

$$J = \sum_{n=1}^{10} M_n^2 + W(r_{l,n} - r_{p,n})^2$$
$$\text{subject to } g(x) < 0$$

M is corrective yaw moment. r_l, r_p, W and $g(x)$ are desired yaw rate from (3), yaw rate developed in (8), weighting, state constraints, respectively. State constraints $g(x)$ can be defined as follow:

$$\dot{\beta} - r: \quad r_{\max} + \dot{\beta}_{\max} = \begin{cases} \dfrac{F_{yr\_\max}(1+\frac{b}{a})}{mv_x} & F_{yf\_\max} \geq \frac{b}{a} F_{yr\_\max} \\ \dfrac{F_{yf\_\max}(1+\frac{a}{b})}{mv_x} & F_{yf\_\max} < \frac{b}{a} F_{yr\_\max} \end{cases} \tag{9}$$

$$\beta - r: \quad -\beta_{\max} + \frac{b \cdot r_{\max}}{v_x} = \alpha_{r\_\max} \tag{10}$$

(9) is defined as in [6] but $\dot{\beta}$ is added to the equation. (10) is determined for the vehicle not to exceed the slip angle which generate the maximum lateral tire force. For the $\dot{\beta} - \beta$ boundary, a look-up table is used for practical reason.

4.4. Distribution of the corrective yaw moment

Fig. 3. shows a vehicle with brake force applied on the front right wheel. To generate the negative corrective yaw moment, front right and front rear wheels could be the places that brake forces to be applied. In case of applying brake force on the rear right wheel on a vehicle in a left turn, lateral force of rear right wheel decreases. Diminished lateral forces of rear wheels are followed by creating positive moment which is undesirable in this case. Whereas, in case of applying brake force on the rear right wheel on a vehicle in a left turn, the lateral force of the front wheel decreases which is followed by increase of the negative corrective yaw moment. Considering friction ellipse effect of the tires, wheels that brake forces to be applied are chosen. The following equations calculate the corrective yaw moments as functions of changes of longitudinal tire forces. The change of lateral force due to additional longitudinal force applied by brake is calculated using the tire model [4].

$$M_{c\_f} = \sin\delta \cdot l_f \cdot \Delta F_y + \cos\delta \cdot tb \cdot \Delta F_x \tag{11}$$

$$M_{c\_r} = tb \cdot \Delta F_x - l_f \cdot \Delta F_y \tag{12}$$

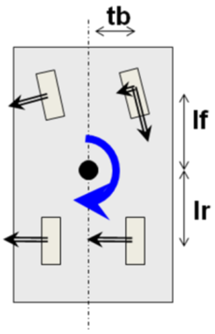

Figure 3. Applying brake force to generate yaw moment

(a) Lateral and longitudinal force vs slip ratio (b) Moment when applying brake on FR (c) Moment when applying brake on RR

Figure 4. Applying brake force to generate yaw moment

In Fig. 4., (a) shows longitudinal and lateral tire forces along slip ratio at a constant slip angle. (b),(c) show generated corrective moments when applying brake forces on the front right and rear right respectively. As shown in (c), the excessive brake force on rear right wheel can generate corrective moment in an opposite direction due to diminished lateral force. The MPC scheme introduces in 4.3 calculates the needed corrective yaw moment. Then, Eq. (11) or Eq. (12) is used to calculate the required brake force using the Newton-Raphson method. The required brake forces are generated by applying proper brake pressure to the vehicle brake system.

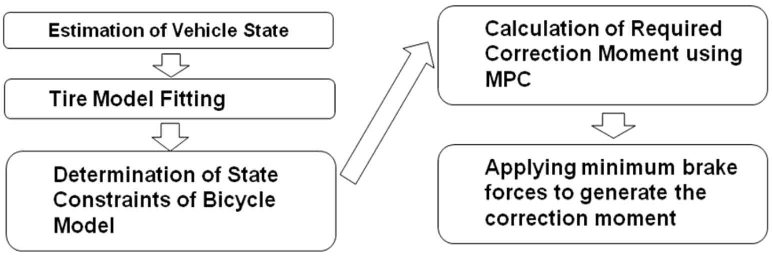

Figure 5. Schematic of the system

5. Simulation Results

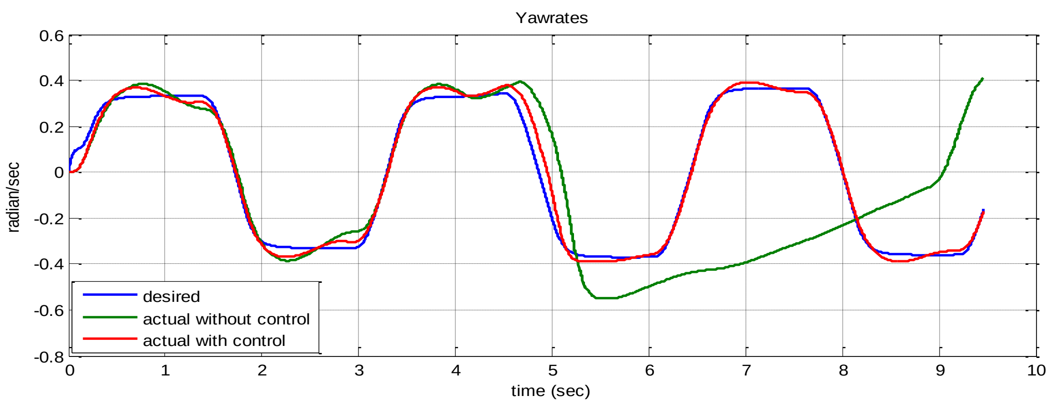

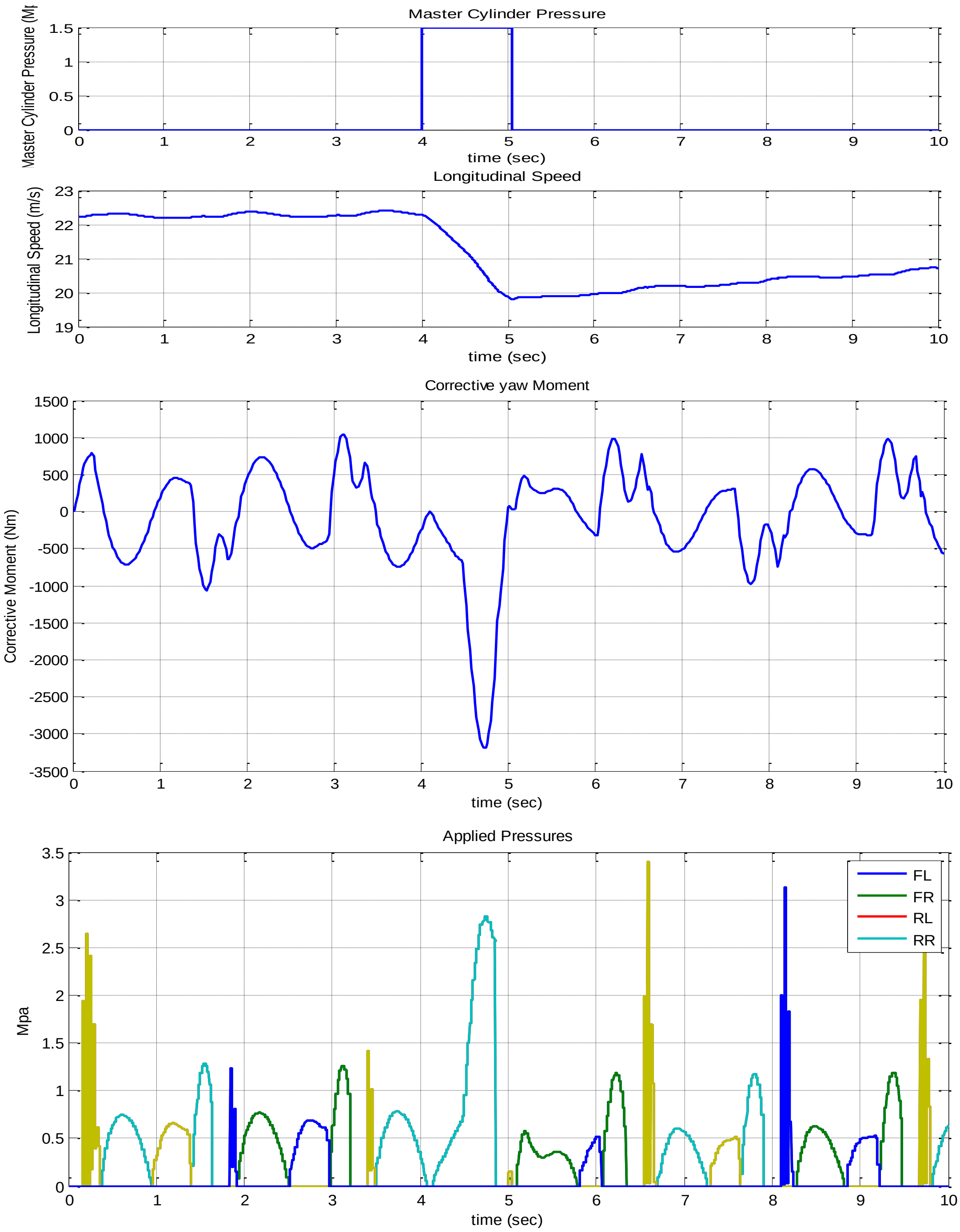

Figure 6. Simulation result

A simulation result using CARSIM is presented in Fig.6. Before the brake pedal is pushed between 4 and 5 second, the vehicle with the control follows the desired yaw rate with less error comparing to the vehicle without any control. After the brake pedal is stepped while turning, the vehicle without control loses it stability and spins out. Whereas, the vehicle with control track the desired yaw rate even when the driver steps on brake pedal while turning.

6. Conclusion

A method of vehicle stability control (VSC) based on MPC is presented. Using the MPC scheme, the proposed controller can actuate brakes to generate correction moment in advance of vehicle being unstable by predicting vehicle movement of several hundred milliseconds ahead. The differences of desired vehicle states from the bicycle model and the estimated vehicle state are minimized by applying the MPC scheme. The simulation result using CARSIM shows that proposed algorithm successfully stabilize the vehicle even brake in a turn is applied to the vehicle.

Acknowledgement

This work was supported by the National Research Foundation of Korea (NRF) grant funded by the Korea government(MEST) (No.2012-0000991)

Reference

1. B.A. Guvenc, T. Acarman, and G. Levent, Coordination of steering and individual wheel braking actuated vehicle yaw stability control, Intelligent Vehicle Symposium, Proceedings of IEEE, 2003, pp. 288–293.
2. W.J. Manning, M. Selby, D.A. Crolla, and M.D. Brown, IVMC: Intelligent vehicle motion control, SAE Trans. 2002-01-0821 (2002).
3. M. Nagai, M. Shino, and F. Gao, Study on integrated control of active front steering angle and direct yaw moment, JSAE 20024250 (2002), pp. 309–315.
4. Y.-H.J. Hsu, S.M. Laws, and J.C. Gerdes. Estimation of tire slip angle and friction limits using steering torque. Control Systems Technology, IEEE Trans-actions on, 18(4):896{907, July 2010.
5. R. Rajamani, Vehicle Dynamics and Control. New York: SpringerVerlag, 2005
6. Craig E. Beal, Applications of Model Predictive Control to Vehicle Dynamics for Active Safety and Stability. PhD thesis, Stanford University, 2011.